IASJ المجلات الاكاديمية العراقية

Tikrit Journal of Pure Science

ISSN: 1813 – 1662 (Print) --- E-ISSN: 2415 – 1726 (Online)

Journal Homepage: http://tjps.tu.edu.iq/index.php/j

A study of mineralized water using geophysical and hydrogeochemical approaches in Khwelen salt ponds, Sangaw, Sulaymaniyah, NE of Iraq

Diary Ali Mohammed Al-Manmi , Bakhtiar Qadir Aziz , Azad Taher Kareem , Halo Abdullah Othman, Sarkhel Hawre Mohammed , Hawbir Ata Karim , Assad Ibrahim Mustafa , Hemin Fareq Muhammed

Department of Geology , University of Sulaimani, Iraq

https://doi.org/10.25130/tjps.v25i5.291

ARTICLE INFO.

Article history:

-Received: 17 / 6 / 2020

-Accepted: 23 / 7 / 2020

-Available online: / / 2020

Keywords:

Resistivity Tomography, karst, Mineralized water, hydrochemistry, Kurdistan

Corresponding Author:

Name:

Diary Ali Mohammed Al-Manmi

E-mail:

diary.amin@univsul.edu.iq

Tel:

ABSTRACT

Groundwater is the main source of Khwelen village for domestic and household purposes, furthermore for salt production via salt evaporation ponds. Electrical Resistivity Tomography (ERT) and hydrogeochemical approaches are used to understand the regime and distribution patterns of different types of mineralized water flowing through several springs and wells in a restricted area does not exceed 0.14 Km^2. The high salty one using for producing salt for more than hundreds of years and the sulfurous one that has bad odder. The area is covered by Fatha Formation which has four types of depositional cycles, two of them are considered as impermeable layers they are claystone and marlstone, the others are Limestone and Gypsum layers that characterized by highly fractured and caverns. The inverse sections of the resistivity imaging showing the occurrence of 22 caves of different sizes and at different depths. They are classified into two groups, 10 cavities detected in the Gypsum layers showing high resistivity ranging from 350 Ohm.m to 1200 Ohm.m, they are most probably making the underground paths of the sulfurous groundwater. The second group is 12 cavities appear in the limestone layers of the Fatha Formation and they are showing very low resistivity ranging from 0.4 Ohm.m to 4 Ohm.m and forming excellent paths of the high salty underground water. ERT shows high applicability for finding the boundary between the saline and sulfurous mineralized water.

The groundwater chemistry is controlled by many overriding factors which are: dissolution, mineral precipitation, cation exchange, and salinization, besides the effects of localized topography, mixing, and geology. These processes are proved from the results of ionic concentrations, saturation indices, HFE diagram, and oxygen and hydrogen stable isotopes.

1-Introduction

The term of mineral water is a specific form of groundwater, from which it varies in its composition and properties. The criteria for differentiation can lie in increased mineral content, elevated carbon dioxide and hydrogen sulphide content, elevated temperature, or the presence of higher concentrations of trace elements such as sulfur, fluoride, iron, iodine, or radon.These types of water have been favored by people from ancient times, whether for drinking or bathing, because such waters usually have, or are associated with, beneficial health properties [1]. Evliya Celebi describes the water cure as follows [2]: "Firstly the curist should not eat salty but should only drink warm water for 3 days. Following this, the curist should drink the mineral water 3 times a day for 3 days and eat unsalted foods. The water cures humors (fluids) of the body (as described by the old physicians)."

In the midst of the Sangaw area exactly at the Khwelen village, is a collection of startling beautiful salt evaporation ponds, creating an amazing landscape. The ponds have several cubic meters with depths of 0.2 m up to 0.5 m, Fig. (1 A). Water is pumped from a well drilled from many decades and its depth is 5 m

and located about 500m to the north of the ponds Fig. (1 B). While crossing through the pond system salinity levels slowly increase as a result of evaporation and sodium chloride precipitates. Since the thirties of the last century, salt was invested by Chamchamal government, and before November 2017, it produced more than 1500 tons of salt. Because of the earthquake that struck in November 2017, production decreased to less than five hundred tons because of mixing freshwater with saline water (self-communication with the villagers). The area is interesting in the hydrogeological point of view, two different types of mineralized water, salty and sulfurous, Fig. (1C) are flowing through several springs continuously for more than hundreds years, even in the extreme drought years 1999, 2000 and 2001 when the average annual precipitation fall from 750 mm to 235, 318, and 410 mm respectively the following of these springs was continuous. Annually thousands ton of salt for domestic uses is produced by evaporation of the saline water. The surface of the area is characterized by the existence of several cavities having different size; most of them were collapsed and filled with the clay, Fig. (1D).

Karsts formed by a combination of high soluble rocks and existing fractures or secondary porosity in an area with unique landforms and hydrological situation. [3]. The vadose zone acquires soil, epikarst, and zone of transmission, anywhere the greatest of the mobilization, moving, and reprecipitation of ions took place [4]. The extension of epikarst zone reaches from 3 m to 30 m and is characterized by high water storage capacity [5, 6, 7, 4). The high porosity and permeability of this zone make this zone to be the source of water storage and producing perched aquifer, moreover feeding the fissures and conduits in cave drip zone [7,4]. The second zone which is the transmission zone has low water storage comparing with the epikarst zone. [7].

Caves are natural openings in the ground that extend beyond the zone of light and large enough to access the entry of man. The cave is occurring in a wide variety of rock types and produced by generally differing geological processes, it ranges in size from small single rooms to interconnecting passages many kilometers long [8]. The process of formation and development of caves is known as speleogenesis. The caves around the world (about 80%) developed by the percolation of rainfall water with a high content of CO_2 (aq) which dissolved carbonate-hosted rocks with a lack of water drainage. [5]. The size, morphology, and hydrology of the karstic cave are controlled by the permeability, hydrogeology, solubility, and structure of the hosted rocks, in addition to the climate characteristics [9].

The study area displays distinctive surface karst features. Where the limestone rock of the Pila Spi formation and gypsum layers of Lower Faris outcrop, common Karren structures such as meandering Karren, panholes or trittkarren are formed caused by solution on these massive bare limestone surfaces. This area is marked by a cumulative occurrence of very deep crevasses and dolines which are frequently described as “diagnostic karst landforms” [10, 3]. In some cases, the murmuring of subterranean rivers can be heard, generally associated with the characteristic foul odor of hydrogen sulfide.

2D resistivity imaging is selected to be used in a restricted area equal to 0.14 km^2 located NE of the village, both mineralized saline and sulfurous water flowing through springs within this area. The study is conducted to find out subsurface paths of both types of mineralized water as well as mapping cavities distribution in more soluble limestone and gypsum rocks. The 2D resistivity imaging also aimed to test the capability of this technique for differentiating between the two different types of mineralized water. Several kinds of research were carried out nearby the current area for evaluating groundwater and detecting cavities filled with freshwater using 2D resistivity imaging such as [11,12]. The study of mineralized water is carried out in different parts of the world by using 2D resistivity imaging such as [13, 14, 15, 16]. Moreover, the hydrogeochemical method is combined with a geophysical method to determine and describe the different water types, which occur in the study area. further, the geological and hydrogeological conditions, which affect the chemistry of the groundwater, were determined.

2-Location of the study area

Khwelen is located in the low mountainous area of the northwest plunge of Azhdagh anticline, about 17 km to the northwest of Sangaw district and about 85 km southwest of Sulaimaniyah City, NE Iraq in Iraqi Kurdistan (Fig. 2). The Khwelen Village is located at the intersection point of the longitude 45° 00′ 04″ E and latitude 35° 22′ 02″ N, the area elevated about 590 m above sea level.

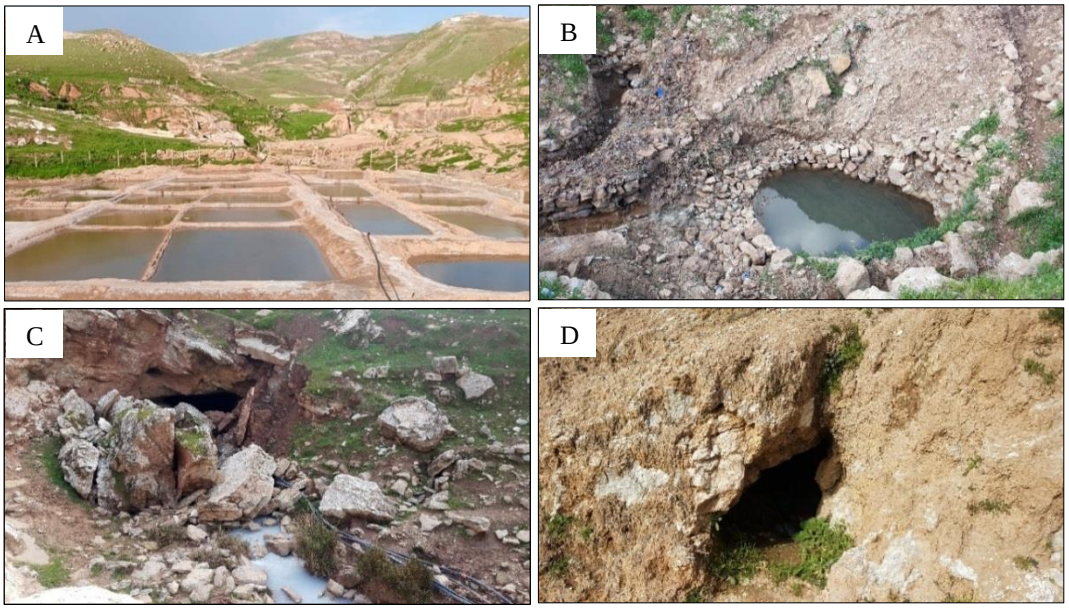

Fig. 1: A. Evaporation salt ponds B. Well feeding the ponds
C. Hydrogen Sulfide Spring D. Sinkhole inside gypsum layer

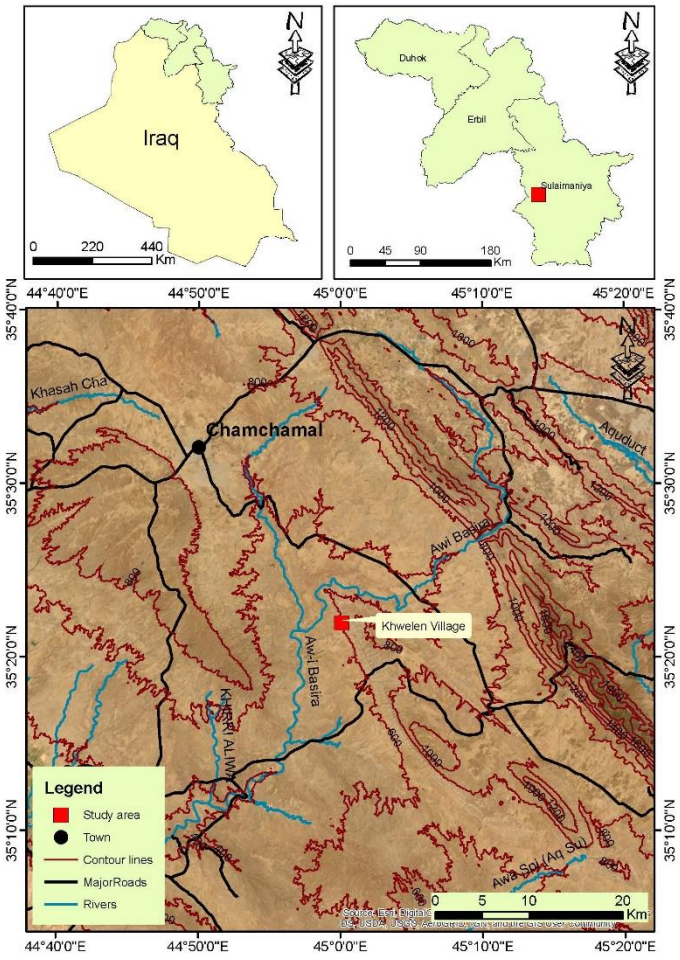

Fig.2: Location map of the study area

3- Geology of the studied area

Geologically many rock units exposed in the study area, which are (Pilas Spi, Fatha, and Injana Formations Fig.(3 and 4).

Pila Spi Formation (Late Eocene) comprises two units, the upper part which comprises well bedded, bituminous, chalky, and crystalline limestones ,with bands of white chalky marl and with chert nodules

toward the top. The lower part comprises well bedded hard porous or vitreous, bituminous, white, poorly fossilifirous , limestones, with algal or shell sections.

There are many Formations exposed in the area belonging to Oligocene according to [17, 18 , 19], as follow:

Sheikh Alas and Shurau Formations belong to the lower cycle and Bajawan, Baba, Tarjil, and Anah Formations belong to the upper cycle. Sheikh Alas comprises porous to highly cavernous, recrystallized limestone layered partially dolomitized with organic-rich in Nummulitic white-milky color limestone beds. While Shurau Formation includes white-grey fossiliferous limestone beds characterized by porous and vugs.

Tarjil Formation consists of hard splintery green to grey Globigerinal marly limestone, the beds partly become marl and friable, the marly limestone beds are dolomitized. While Baba Formation White comprises massive, highly jointed, fractured, porous partially dolomitized and fossiliferous limestone bed of chalky appearance and groovy surface. The Bajawan formation composed of white-milky color, highly jointed and cavernous, fossiliferous limestone, characterized by a highly porous sieve structure formed as a result of the dissolution process, with interbeds of thin marl beds. Moreover, Anah formation composed of White-creamy and grey dolomitized and recrystallized- brecciated limestone bed while the upper part includes rubbly, conglomeratic limestone, and conglomerate bed.

According to [20] the Fatha Formation (Middle Miocene-Tortonian) consists of four units (from the bottom to the top are: The transition beds, which are comprised mostly of anhydrite separated by thin limestones and mudstone. The Saliferous beds are made of rock salt and anhydrite with siltstones, mudstone, and some limestone intercalation. While the fourth named seepage beds comprised anhydrite with any siltstones and limestone beds. The upper red beds composed of reddish mudstones and siltstones with relatively limestone and anhydrite. In the studied area, the formation is composed of a cyclic repetition of gypsum, marl, red claystone, and specific interbed of limestone and sandstone [21]. Khwelen village located on the Fatha Formation. The thickness of the formation in the well CH.2 in Chamchamal is 448m [22, 23). The formation in CH.2 consists of four members; upper red bed 161m, seepage bed 40m, saliferous bed 136 m, and transition bed 111m

Injana Formation (Late Eocene) comprises fine-grained pre-molase sediments, the basal units comprise thin-bedded calcareous sandstone and red and green mudstones with one thin gypsum beds and a purple siltstone horizon with glass shards [24]. Its lower contact is gradational with Fatha Formation and the upper contact is gradational with Mukdadiya Formation characterized by the presence of gravely sandstone. Fatha and Injana formations formed the flank of Azhdagh anticline.

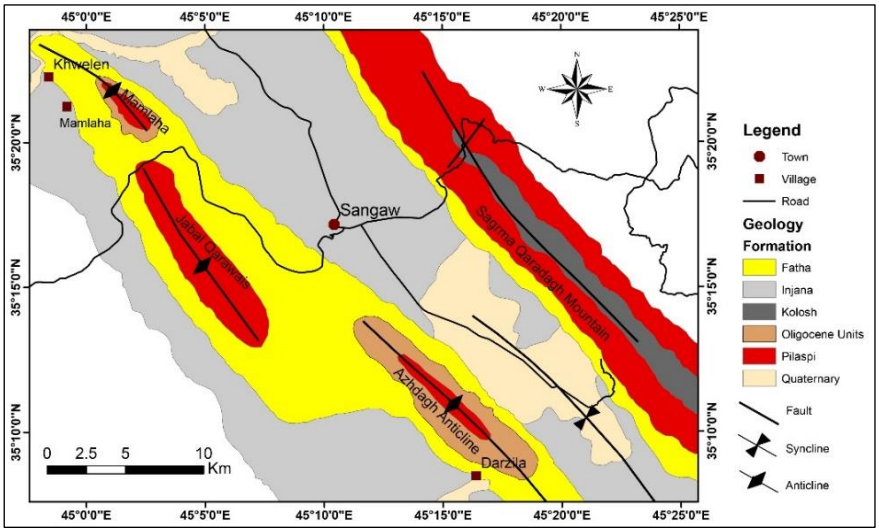

Fig.3: Geological map of the study area (Adapted with permission from 21)

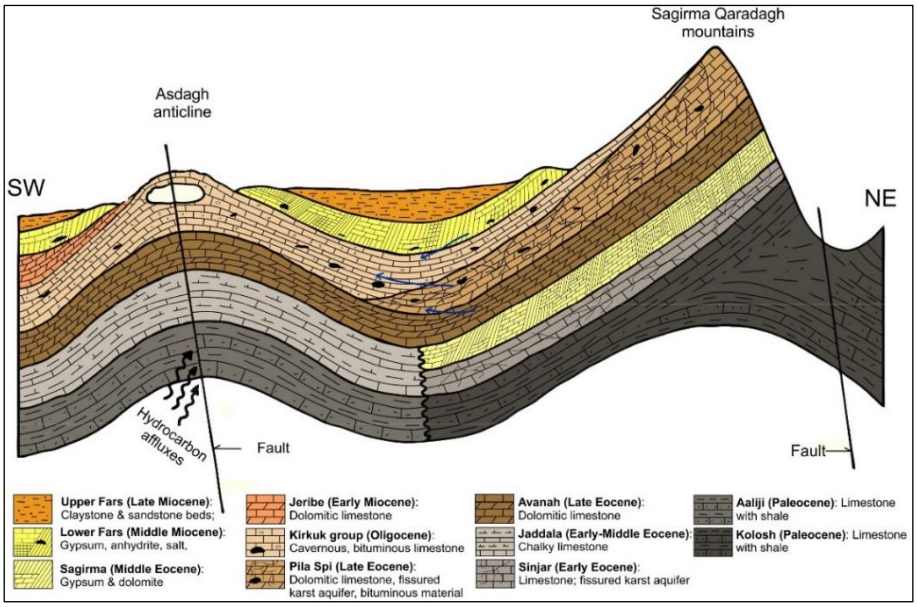

Fig.4: Geological cross section from southwest to the northeast of the study area (Adapted with permission from 25)

4- Climate and hydrogeology

The climate of Kurdistan is characterized by extreme conditions, wherever a large variety in temperature within day and night and between winter and summer are observed. This significant difference in the temperature is usually expressed as climate extreme. This extreme characteristic is one of the main conditions of the continental climate [23].

According to the climate data of Chamchamal Station, the average annual rainfall of the area is 463 mm. The maximum rainfall drops in January 99 mm. The monthly average temperature is 19.9 °C. The average annual relative humidity is 42.7 %. The area is characterized by a high amount of evaporation with 1977mm/year.

Hydrologically the study area is located in Chamchamal- Sangaw basin. The main aquifer system is Pila Spi aquifer which is highly fissured, well-karstified in the core of Ashdagh anticline and local aquifer system in Oligocene rocks with many features, channels, and caves that can be observed on the surface. Pila Spi consists of Eocene limestone, sometimes up to 200 m thick, and represents a typical heterogeneous anisotropic aquifer that is fractured and intensively karstified [26]. The aquifer contains medium to large groundwater reserves strongly varying in space and time. As a result of general aquifer anisotropy and the presence of many fissures, the aquifer is generally characterized by a very high permeability [26].

The values of transmissivity are in the range of 3.5 to 42000 m²/day [25, 27]. The recharge rate of Pila Spi karstic aquifer from the rainfall is high due to the effective infiltration capacity of the rocks.

The evaluation of the infiltration rate depends on the existence of the high fracture and karstified rocks, depressions, dolins, and the absence of vegetation. Throughout the wet season, the decreased evaporation rate, high rainfall, and also the slope contributes to the stated rate of the "Pila Spi" aquifer. Meteoric water infiltrating through Pila Spi, Oligocene rocks, and Fatha Formations layers enriched in sulfate, therefore, the Pila Spi aquifer gradually enriched more sulfate along the flow path of groundwater. Lower and Upper Fars Formations are less productive water-bearing layers that are tapped by wells and are characterized by poor water quality because of evaporites leaching [28].

Several springs appear in the study area, they are perennial everywhere the year which depends on the runoff duration although they differ with the daily discharge volume as reported by [29]. Hydrochemically the springs characterized by the high content of dissolved ions and most of them are sulfide springs.

5- Methodology

5.1- The resistivity tomography data acquisition method

Electrical resistivity tomography (ERT) is selected for investigation of the area under consideration, this is depending on the geological and structural situation of the area. Besides, the main goal of the study which is detecting and differentiating between two types of mineralized water, saline, and sulfurous waters, needs a high-resolution geophysical method. The type of resistivity meter was Syscal-72 R1 Plus. The survey carried by using Wenner-Schlumberger array and the electrode spread equal to 5 m so that the length of each profile was 355m.

Four profiles were laid out, Fig. (5), two of them running approximately parallel to the strike of the outcrops and the other two are running normal to the strike. The software package "RES2DINV" version 3.59.117 is used for 2D model analysis and interpretation. It performs smoothness-constrained

inversion using finite difference forward modeling and Quasi-Newton techniques [30].

5.2- Hydrochemical method

A field survey was conducted in January 2019 for collecting water samples and checking the prevailing situation. Four sites were collected for sampling, two wells, and two springs. Polyethyleneusing 250 ml bottles were used for collecting water samples for major element analysis and then the samples were filtered by a 0.2 µm filter paper to get cleared of colloids. The physical parameters temperature, electrical conductivity (EC), and pH were measured in situ using AP 85 and AP 75 Fisher Scientific Analyzer devices. Hydrogen sulfide is stabilized in the field by applying [31 and [32] standard procedure using 1 L bottle sample. The test is performed by titrating the excess of Iodine with sodium thiosulfate by using a starch indicator [33, 34].

The water samples were analyzed at the laboratory of Sulaymaniyah Health Protection Directorate following the American Public Health Association [35] standard procedure using titration and photometry. An analytical error of the analysis performed using a charge balance method, the results showed that the analysis is within the acceptable range which is below 5%. Aq. QA, v.1.1 software was used for plotting the chemical data of water samples on the Piper diagram.

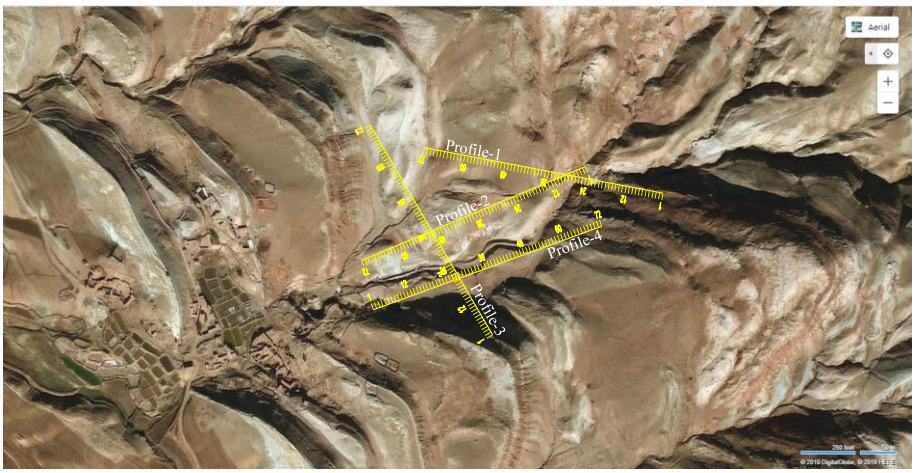

Fig. 5 Satellite image showing the geoelectric survey profile

6- Results and discussion

6.1- Geoelectrical resistivity and VES investigations

-Profile 1

It is running N78W, the length of the profile is equal to 355 m. Good data quality is obtained as it is observed from the similarity between measured and calculated apparent resistivity sections as shown in Fig (6). The inverse model resistivity section of the sounding show's appearance of several zones has varied resistivity magnitude due to different lithological components of the FathaFormation. Zones of high resistivity ranging from 300 Ohm.m to 1400 Ohm.m most probably represent the Gypsum layers of the L.F Formation. Four cavities within this layer are identified and characterized by the existence of sulfurous water. They are detected beneath electrodes 20, 33, 53 and 59, the first one (I) is small has a length of about 10 m and width 7 m, it is located at depth of about 7.5 m. The second cave (II) filled with sulfurous water has dimension equal to 20m x 27 m and it is located at depth equal to 17 m. The third (V) and fourth (VI) caves have a dimension of 11 m x 4 m and located at depths near to 14 m and 20 m respectively.

Very low resistivity ranging from 1 Ohm.m to 5 Ohm.m recorded in three locations. They are representing cavities filled with salty water detected in the limestone rocks of the L.F Formation. The cave (III) has a dimension of about 12 m x 9 m, located beneath electrode 16 and a depth of 23 m. A small cave (IV) its dimension equal to 4 m x 11 m is detected below electrode 29 at depth equal to 13 m.

-Profile 2

It is running normal to the strike of the outcrops, the inverse model resistivity section, Fig. (7), of the sounding shows also the appearance of several zones that have varied resistivity magnitude. It is due to different lithological components of the L. F. Formation as well as caves filled with saline water and others filled with sulfurous water. Gypsum layers of high resistivity are detected, its resistivity ranging from 250 Ohm.m to 1100 Ohm.m most. Within gypsum layers, two caves are detected, the large cavity (I) is detected at depth 8 m and beneath electrode 35, it is filled with sulfurous water and has a dimension equal to 15 m x 13 m. The second caves (II) is located beneath electrode 49 at depth nearly 12 m, it has a dimension of about 10 m x 5 m.

Two small caves, (III) and (IV), are detected in the limestone layers, they are showing very low resistivity ranging from 1.5 Ohm.m to 4 Ohm.m. The cave (II) has a dimension equal to 17 m x 4 m, located beneath electrode 22 and a depth of 13 m. The second cave (III) has a dimension equal to 20 m x 11 m is detected below electrode 64 at depth nearl to 13 m.

-Profile 3

It is running parallel to the strike of the layers, the length of the profile is equal to 355 m. The inverse model resistivity section, as shown in Fig. (8), of the sounding show's appearance of several zones either have very high resistivity or very low resistivity. The high resistive Zones related to caves in gypsum layers filled with sulfurous mineralize water while the very low resistive zones refer to the caves in limestone layers filled with salty water. Three caves were detected showing high resistivity ranging from 400 Ohm.m to 1000 Ohm.m. The first one (I) is small has a length equal to 17 m and width equal to 3 m, it is located at a depth of 13 m below the electrode 36. The second cave (II) filled with sulfurous water has dimension equal to 10 m x 18 m and it is located at depth near to 19 m below the electrode 55. The third cave (III) has a length of about 12 m and width equal to 2.5 m, it is located at a depth of 5 m below the electrode 61.

Very low resistivity ranging from 0.8 Ohm.m to 3 Ohm.m recorded in two locations. They are representing cavities filled with salty water detected in the limestone rocks of the L.F Formation. The cave (IV) has a dimension equal to 13 m x 2 m, and it is located beneath electrode 19 and a depth of 12 m. The second low resistive cave (V) has a dimension near to 6 m x 7 m is detected below electrode 25 at depth of about 13 m.

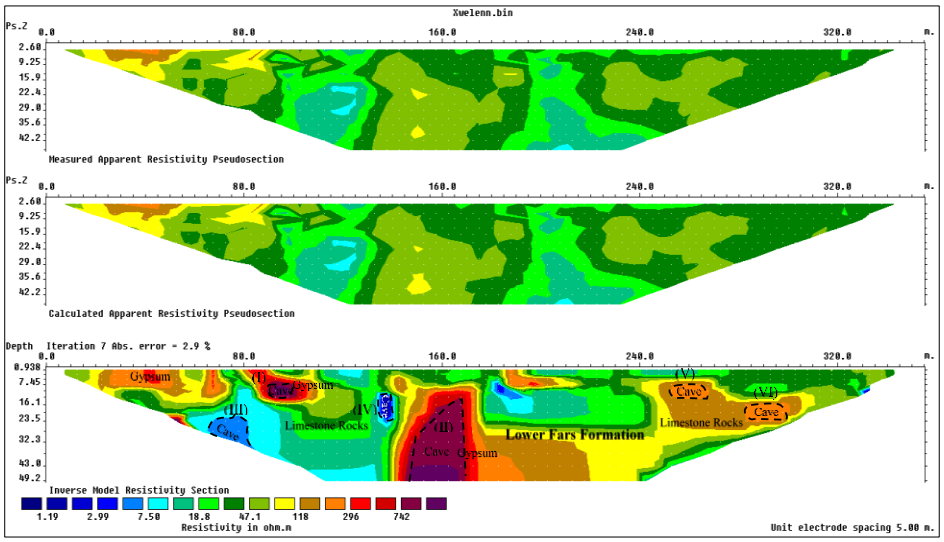

Fig. 6: Interpretation of the 2D sounding of the profile 1

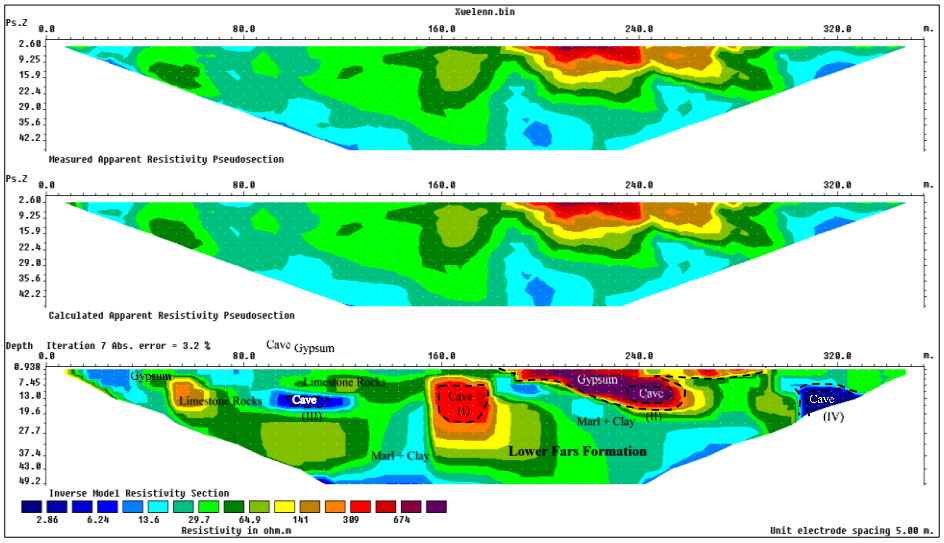

Fig. 7: Interpretation of the 2D sounding of the profile 2

Profile 4

The direction of this profile is N52E and it is running across the trough of the main valley, the mainspring of the salty water is springing near the electrode No.1. The inverse model resistivity section, as shown in Fig. (9), shows an interesting image of the subsurface in this location. A series of small caves detected at depths ranging from 7 to 13 meters, they represent a subsurface gallery for movement of salty water toward the location of the main spring.

Six caves were detected showing very low resistivity ranging from 0.4 Ohm.m to 4 Ohm.m. five of them are small, (I), (II), (III), (IV) and (V), they appear beneath electrodes 17, 21, 32, 39 and 47 and at a

shallow depth does not exceed 13 m. The caves numbered (VI) is the largest one detected in the area; it has occurred at depth near to 13 m below electrode No. 54. This cave has a dimension near to 25 m x 32 m, it is filled with salty water and most probably can be considered the main provider of the saline water to the small caves to flow finally to the main spring.

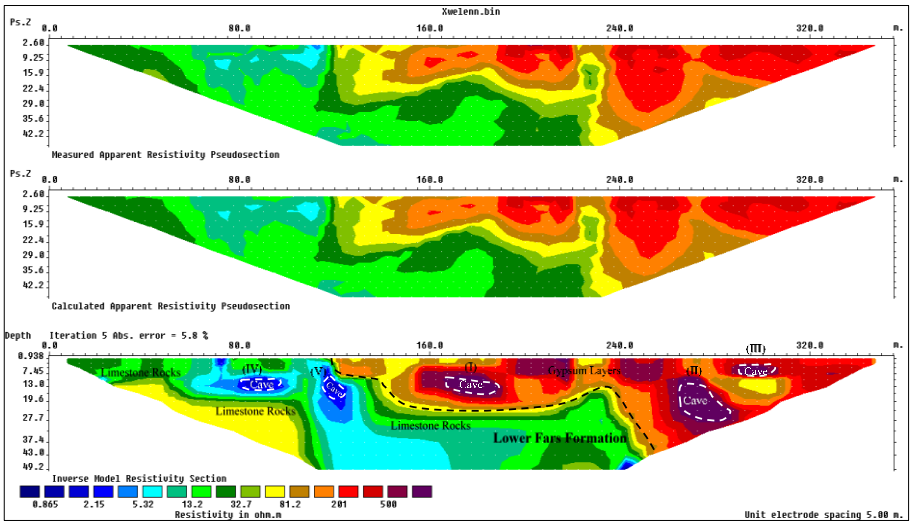

Fig. 8: Interpretation of the 2D sounding of the profile 3

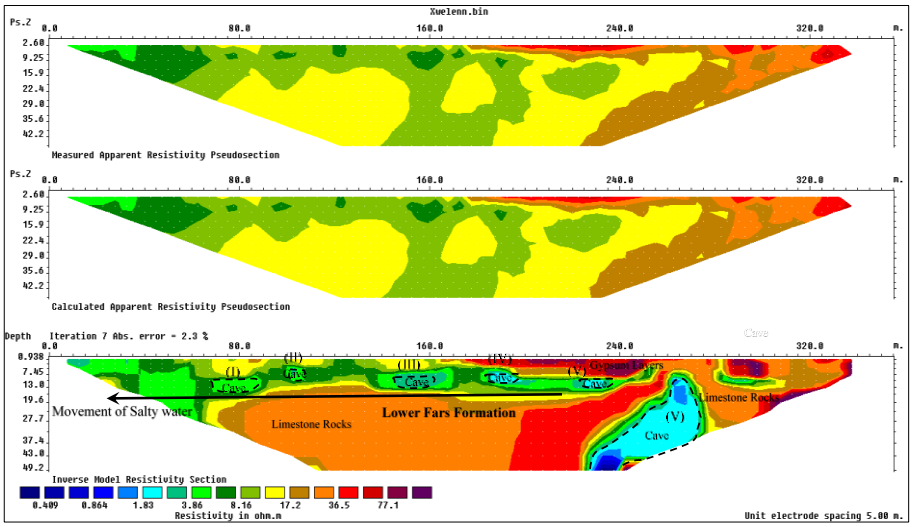

Fig. 9: Interpretation of the 2D sounding of the profile 3

ERT has proven its high applicability for finding the boundary between the saline and sulfurous mineralized water. The main reason is due to the low resistivity of the saline water regarding the higher resistivity of the sulfurous water as well as the existence of the saline water in the low saturated limestone rocks and sulfurous water in the high resistive gypsum layers.

The results show that the potential zone of saline groundwater is in the southwest part of the studied area, Fig (10), while the potential zone of sulfurous groundwater is located in the northeast part of the area.

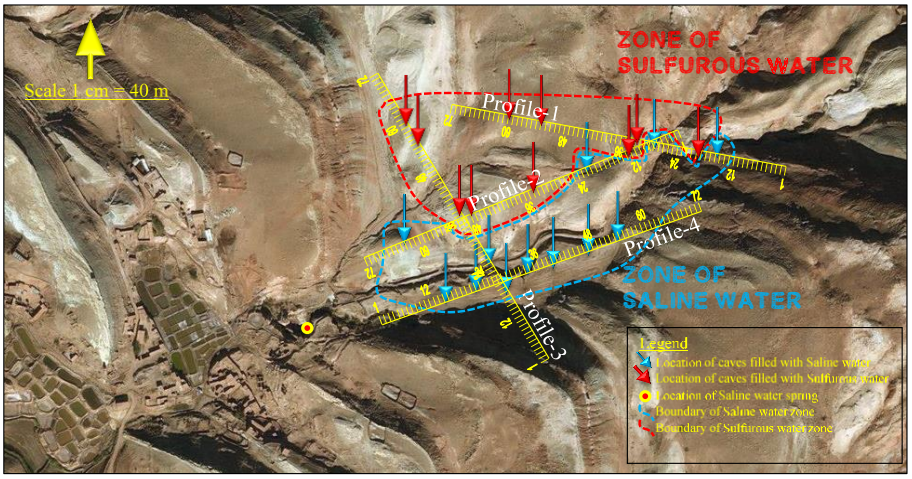

Fig. 10: Shows the Interpretations of 2D sounding profiles

6.2- Hydrochemistry

A. Major anions and cations

The results of physiochemical parameters are presented in Table 1 and displayed in Fig. (11). The sample W1 indicates exceptionally high concentration levels compared to the other sampling sites and the TDS value of this site is 10202 mg/L. The dominant cation and anion are Ca^{2+} and SO_4^{2-} except in sample W1 the dominant anion is Cl^-. The concentrations of Ca^{2+}range between 265 mg/L to 664 mg/L and for SO_4^{2-} range between 385 mg/L to 1400 mg/L. Other predominant ions are Mg^{2+}, Na^+, Cl^-, and HCO_3^- ions. The relatively high concentration of (Ca^{2+}, SO_4^{2-}) is expected to be issued from gypsum layers of the Lower Faris rocks.

According to the major cation and anion results and Piper diagram plot of the water samples, two different water types are identified in the area of interest, these are NaCl, and $CaSO_4$, Fig. (12). Based on the stable isotope data ($\delta\ ^2H$ and $\delta\ ^{18}O$) which was carried by [25] in the Darzilla vicinity area, about 30km, it indicates that all samples plot on or slightly below the Eastern Mediterranean meteoric water line. Therefore, the recharge is affected partially by evaporation in some areas. Besides the rapid recharge take place in other areas, possibly via preferred pathways especially via the joints and fractures, limiting any notable evaporation.

The groundwater predominant anion type change from sulfate to chloride beside an increase of total dissolved solids. This is usually attributed to the comparative age and groundwater path length and low groundwater flow [36]. When the static regime of groundwater appears the NaCl type waters exist (i.e. the lower-lying areas). An Additional intermediate type of water will be generated as a result of some hydrogeochemical process between ($CaSO_4$ and NaCl) end-member. The $Ca(HCO_3)_2$ waters type produced by carbonate minerals dissolution via interaction between enriching surface water with atmospheric and biogenic CO_2 and ultimately infiltrates into the underground. The development of $Na(HCO_3)_2$ waters is formed by cation exchange between calcium and sodium. When the carbonate minerals are precipitated, the calcium is removed from the solution and this may change the chemical equilibrium which result in the dissolution of gypsum that contains calcium, Therefore, $CaSO_4$ type waters develop [37]. The Ca ion is removed from the solution by cation exchange processes and bound Na to form Na2SO4 waters. Sulfate reduction of $CaSO_4$ and Na_2SO_4 waters leads to the formation of $Ca(HCO_3)_2$ and $NaHCO_3$, sequentially. Continuous sulfate reduction is shown in the water samples by the presence of H_2S. Groundwater in the area is characterized by a nasty smell produced by sulfate-reducing bacteria, which change sulfate into H_2S. The formation of NaCl and $CaCl_2$ waters is a result of progressive salinization of the waters. At higher salinities, the process of reverse cation exchange may create $CaCl_2$ waters due to the removal of Na out of solution for bound Ca. Alternatively, $CaCl_2$ type waters could also be a result of the process of mixing between a “younger”, fresher water with more saline older water.

Table 1: Physio-chemical properties of Khwelen Water samples

Parameter	Units	W1	W2	S1	S2	Average
T	^{o}C	20.2	20.4	20	21.6	20.5
pH		6.98	6.1	7.8	6.98	7.17
EC	µs/cm	15940	2760	1757	3430	5972
Pe	milivolt	-22.7	-6.3	57.1	-15.2	3.23
TDS	mg/L	10202	1766	1124	2195	3821
Ca^{2+}	mg/L	664	415	265	532	469
	meq/L	33.2	20.75	13.25	26.6	23.5
	% meq/L	13.6	48.4	54.2	50.3	41.6
Mg^{2+}	mg/L	477	225	110	235	262
	meq/L	39.75	18.8	9.2	19.6	21.8
	% meq/L	16.2	43.7	37.5	37	33.6
Na^{+}	mg/L	3950	75	45.3	152	1056
	meq/L	171.7	3.26	1.97	6.61	45.9
	% meq/L	70.14	7.6	8.1	12.5	24.6
K^{+}	mg/L	6.8	5.6	2.2	5.1	4.9
	meq/L	0.17	0.14	0.06	0.13	0.13
	% meq/L	0.07	0.33	0.23	0.25	0.22
Sum of Cations	mg/L	5098	720.6	422.5	924	1791.3
	meq/L	244.9	42.9	24.4	52.9	91.3
	% meq/L	100	100	100	100	100
SO_4^{2-}	mg/L	1400	650	385	940	844
	meq/L	29.2	13.5	8.0	19.6	17.6
	% meq/L	21.1	59.4	54.6	66.7	50.4
Cl^{-}	mg/L	3750	120	75	145	1023
	meq/L	104.2	3.3	2.1	4.0	28.4
	% meq/L	75.2	14.6	14.2	13.7	29.4
HCO_3^{-}	mg/L	320	362	280	350	328
	meq/L	5.25	5.93	4.6	5.74	5.4
	% meq/L	3.8	26	31.2	19.6	20.2
CO_3^{2-}	--	0	0	0	0	0
Sum of Anions	mg/L	5470	1132	740	1435	2194.3
	meq/L	138.6	22.8	14.7	29.4	51.4
	% meq/L	100	100	100	100	100
H_2S	mg/L	0	3.2	4.8	7.3	3.8

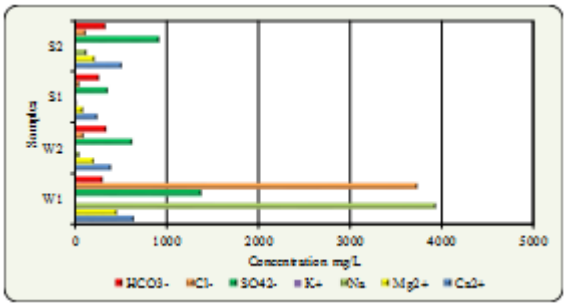

Fig. 11: Main cations and anions of the samples

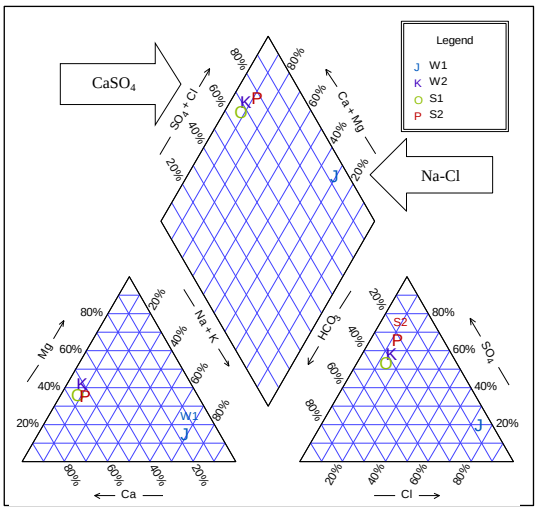

Fig.12: Piper diagram showing the different water types in the study area

6.3- Hydrogen sulfide

The concentration of H_2S ranges from zero in sample W1 to 7.3 mg/L in sample S2 with an average of 3.8 mg/L.

Hydrogen sulfide typically originates either from oil-rich reservoirs directly or from the reduction of sulphates by organic matter [38], as shown in this representative but unbalanced reaction:

$$SO_4^{2-} + H_2O + 2[C] \xrightarrow{\text{Anaerobic Bacteria}} 2HCO_3^- + H_2S \quad \text{.....(1)}$$

$$CaSO_4 + H_2O + 2[CH_2O] \longrightarrow CaS + 2CO_2 + 2H_2O \quad \text{.....(2)}$$

$$CaS + CO_2 + H_2O + \longrightarrow CaCO_3 + H_2S \quad \text{.....(3)}$$

The expression [C] is symbolic of an organic compound. Theoretically, thermochemical sulfate reduction (TSR) without any microbiological support may occur at temperatures as low as 25 °C [39]. However, only at temperatures above 100-140 °C reaction rates appear to be high enough to be geologically significant. At temperatures less than about 80 °C the reaction requires bacterial mediation (bacterial sulfate reduction = BSR) [40,27, 34].

Heiland, 2012 who worked on Darzila cave which is far about few kilometers from the current study area was "mentioned that the cave sulfur is thought to originate from petroleum fields or gypsum layer of FathaFormation. A small oil spill into Awa Spi river confirms the general presence of hydrocarbons. The occurrence of substantial oil reservoirs in the vicinity of the cave is not documented in the literature. However, only about 5 km from the cave, confidential test drillings are performed. Furthermore, the Chamchamal and the Khor Mor gas-condensate field, as well as the famous Kirkuk oil field are located within a few tens of km distance from the study area".So the same situation is valid for the Khwelen village, the layer of gypsum is the main source of Sulphur.

6.4- Saturation indices calculation

The calculation of water saturation degree with respect to solid mineral phases can be reached as in the following equation [41]:

$$SI_x = \log \frac{IAP(T)}{KSP(T)} \quad \text{.....(2)}$$

Where

SIx*: is* the saturation index of mineral x,

IAP (T): is the ion activity products at a specified temperature (^oC)

and Ksp: is the equilibrium solubility product constant of mineral x.

A computer program *WATEQ4F* [42] is used for calculating speciation for water samples, the results are tabulated in Table (2).

Generally, there are only minor differences between the water samples in the number of under- and supersaturated solutions with regard to the given minerals. [43] mentions that the dissolution rate is greatest at or near the water table because oxygen is most abundant in the open air, for example, the site S2 where the spring emerges from a cave. Due to this fact, most cave rooms are widest at the present or former levels of the cave water [43].

It is obvious from the results that all water samples are supersaturated with respect to Aragonite, Calcite, and Dolomite minerals, while all samples are undersaturated with respect to Anhydrite, Gypsum, and Halite minerals.

According to [44] precipitation and dissolution of carbonates are, amongst others, influenced by kinetic effects in relation to the release of CO_2. If CO_2 degasses into the atmosphere the capacity for dissolution of limestone is decreased. The source of Anhydrite, Gypsum, and Halite minerals are from Lower Faris formation, and the undersaturation state that the caves in the study area still are enlarging and collapsing of the land is noticeable in most of the study area, Fig. (1C).

Table 2: The output of *WATEQ4F* program for Khwelen water samples

Ref.	Ionic Strength	Log P_{CO2}	Saturation indices					
			Aragonite	Calcite	Dolomite	Anhydrite	Gypsum	Halite
W1	0.2221	-1.65	0.1	0.25	0.65	-0.63	-0.4	-3.6
W2	0.0461	-1.46	0.12	0.27	0.57	-0.77	-0.53	-6.7
S1	0.0282	-2.45	0.77	0.92	1.75	-1.02	-0.79	-7.1
S2	0.0558	-1.55	0.26	0.40	0.76	-0.57	-0.33	-6.33

6.5 -Hydrochemical Facies Evolution (HFE) diagram

The HFE diagram that is proposed by [45] is applied to data from Khwelen village to determine hydrochemical facies evolution Fig. (13). In the diagram the abscissae represent, separately, the percentages of Na^+ and Ca^{2+} in meq/L, reproducing the base exchange reactions. The ordinates represent the percentages of anions: the percentage of chloride represents seawater and the percentage of bicarbonate or sulfate (depending on the dominant anion in freshwater) characterizes the recharge water. A spreadsheet software package used which is proposed by [46] The result shows that there are three facies (Na-Cl, $MixCaSO_4$, and $CaSO_4$), Table (3). The results revealed that some parts of the aquifer are recovering during the recent water recharge. The presence of water with a sulfate facies means that the recharge waters can be either bicarbonate or sulfate type.

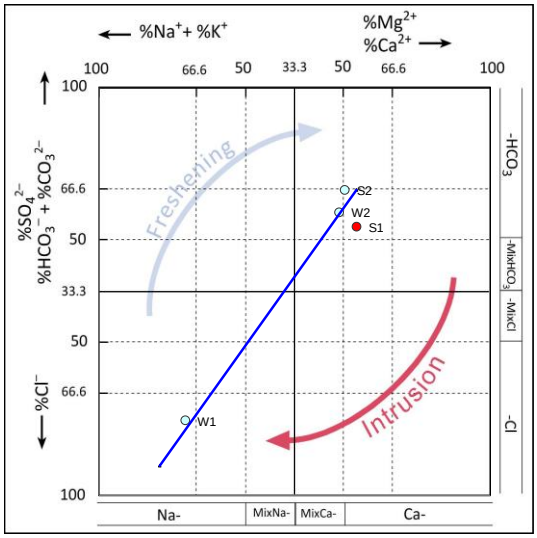

Fig. 13: Hydrochemical Facies Evolution Diagram (HFE-D) of water samples

Table 3: Phases and facies of water samples in the study area

Ref.	Ca^{2+}	Mg^{2+}	Na^+	K^+	HCO_3^-	SO_4^{2-}	Cl^-	Phase	Facies
W1	664	477	3950	6.8	320	1400	3750	Fresh.	NaCl
W2	415	225	75	5.6	362	650	120	Fresh.	$MixCaSO_4$
S1	265	110	45.3	2.2	280	385	75	Intrus.	$CaSO_4$
S2	532	235	152	5.1	350	940	145	Fresh.	$CaSO_4$

7- Conclusion

The application of ERT in this study was to conclude whether it can capable to differentiate between two types of mineralized water close to each other in an area not exceeds 0.14 km^2, besides, the survey carried out on a rough topography, complex geological situation and highly caverns area. The study proved that ERT active for solving such types of problems and it has high resolution to map subsurface situations in the hydrogeological point of view. The ERT is very effective to detect and identify very close caves either filled with saline water or filled with sulfurous water.

Through the current study, about 20 caves of different sizes and depths were detected. They are classified into two groups, 8 cavities detected in the Gypsum layers showing high resistivity ranging from 350 Ohm.m to 1200 Ohm.m, and they are forming the underground path of the sulfurous groundwater. The second group is 12 cavities appear in the limestone layers of the Fatha Formation and they are showing very low resistivity ranging from 0.4 Ohm.m to 4 Ohm.m and forming an excellent path of the high salty underground water.

The hydrochemical approach for this study revealed that the groundwater in the Khwelen area categorizes into two types, NaCl and $CaSO_4$ type. Based on the hydrochemical data and HFE diagram, the controlling factors of hydrogeochemical properties of groundwater are dissolution- precipitation, ion exchange and mixing.

From the previous stable data, it concludes that the groundwater is being recharged by rainfall which enriched with biogenic carbon dioxide and when entering the aquifer it dissolves the soluble salts and minerals and later mix with soluble gypsum to generate sulfate water type, furthermore the dissolution of saliferous bed in Fatha Formation enriched the water with Na and Cl ions.

The earthquake that struck the Kurdistan region in November 2017 has a great effect on the quality of the water, the electrical conductivity dropped down comparing with a previous study that conducted in 2001 due to mixing water has fewer contents of dissolved minerals with saline water.

References

[1] Caballero, B., Trugo, L. and Finglas, P. (2003). Encyclopedia of food sciences and nutrition: Volumes 1-10. Encyclopedia of food sciences and nutrition: Volumes 1-10., (Ed. 2):6000 pp.

[2] Reman, R. (1942). Sifali sulari kullanmak ilmi Balneologi ve şifalı kaynaklarımız, Istanbul, Cumhuriyet matbaası:549 pp.

[3] Ford, D. and Williams, P.D. (2013). Karst hydrogeology and geomorphology. John Wiley & Sons:1074 pp.

[4] Frisia, S. and Borsato, A. (2010). Karst in Alonso-Zarza, A.M. and Tanner, L.H (Eds.) Carbonates in continental settings. Elsevier, Amsterdam: 269-318.

[5] Gunn, J. (2004). Encyclopedia of caves and karst science, Fitzroy Dean, New York:1940 pp.

[6] Williams, P. W. (1983). Speleothem dates, Quaternary terraces and uplift rates in New Zealand, Nature, 298: 257-260

[7] Williams, P. W. (2008). The role of the epikarst in karst and cave hydrogeology: a review, *International Journal of Speleology*, **27**:1-10. DOI: http://dx.doi.org/10.5038/1827-806X.37.1.1.

[8] White, W. B. and Culver, D. C. (2005). Cave definition of, in Encyclopedia of Caves, Eds. Culver, D. C. and White, W. B., Elsevier Academic Press, London, United Kingdom: 674 pp.

[9] Alonso-Zarza, A. M., Martín-Pérez, A., Martín-García, R., Gil-Peña, I., Meléndez, A., Martínez-Flores, E., Hellstrom, J. and Muñoz-Barco, P. (2011). Structural and host rock controls on the distribution, morphology and mineralogy of speleothems in the Castañar Cave (Spain). *Geological Magazine*, **148 (2)**: 211-225.
DOI: https://doi.org/10.1017/S0016756810000506.

[10] Bell, F. G.; Waltham, T.; Culshaw, M. (2005). Sinkholes and subsidence. Karst and cavernous rocks in engineering and construction. 1st ed. Berlin: Springer-Verlag:405 pp.

[11] Aziz, B.K. (2005). Electrical Imaging: 2D Resistivity Tomography as a tool for groundwater studies at Mahmudia Village, West Sulaimani City, Iraqi Kurdistan Region, *Journal of Zankoy Sulaimani- Part A (JZS-A)*, **8(1)**:7-16.

[12] Aziz, B.K., and Baban, E.N. (2013). Karst cavity detection in carbonate rocks by integration of high resolution geophysical methods, *Journal of Zankoy Sulaimani- Part A (JZS-A)*,**15(1)**:159-171.

[13] Yalcin, T., Özürlan, G. and Cekirge, N. (2007). Hydrogeochemical and geophysical investigation of the Istanbul Tuzla–Icmeler spring area for environmental and land use planning purposes. *Environmental monitoring and assessment*, **132(1-3)**:125-140. DOI:https://doi.org/10.1007/s10661-006-9508-y.

[14] Boiero, D., Godio, A., Naldi, M. and Yigit, E. (2010). Geophysical investigation of a mineral groundwater resource in Turkey. *Hydrogeology journal*, **18(5)**:1219-1233. DOI: 10.1007/s10040-010-0604-2.

[15] Nordiana, M.M., Bery, A.A., Taqiuddin, Z.M., Jinmin, M. and Abir, I.A. (2018), April. 2-D electrical resistivity tomography (ERT) assessment of ground failure in urban area. *In Journal of Physics: Conference Series*, **995(1)**: 012076.

[16] Costall, A., Harris, B. and Pigois, J.P. (2018). Electrical resistivity imaging and the saline water interface in high-quality coastal aquifers. *Surveys in geophysics*, **39(4)**:753-816.
DOI:https://doi.org/10.1007/s10712-018-9468-0

[17] Kharajiany S. O. A. (2008). Sedimentary facies of Oligocene rock units in Ashdagh mountain-Sangaw district- Kurdistan region-NE Iraq, M.Sc. thesis, University of Sulaimani, Sulaymaniyah, Iraq: 116 pp.

[18] Kharajiany S. O. A. (2013). The Middle Oligocene Rock Strata (Tarjil Formation) in Ashdagh Mountain, Sangaw District, Sulaimani Governorate, Kurdistan Region , NE Iraq. *Journal of Zankoy Sulaimani- Part A (JZS-A)*, **15(3)**.

[19] Kharajiany S. O. A. (2014). Occurrence of early and middle Miocene rocks (Euphrates, Dhiban and Jeribe Formations) in Ashdagh Mountain, Sangaw area, Sulaimanyah vicinity, NE Iraq. *Iraqi Bulletin of Geology and Mining*, **10(1)**:21-39.

[20] Jassim, S. Z. and Guff, J. C. (2006). Geology of Iraq. Jassim (Eds.) D. G. Geo Survey. Min. Invest. Publication. 445 pp.

[21] Khanaqa, P.A. and Al-Manmi, D.A. (2011). Hydrogeochemistry and geomicrobiology of Darzila spring in Sangaw, Sulaimaniyah, NE Iraq. *Iraqi Bulletin of Geology and Mining*, **7(3)**:63-79.

[22] Al-Mirally, T. H. (2006). Study of geophysical evidences to define properties of some structures at low folded zone in Kurdistan Region-Iraq**,** M.Sc. Thesis, University of Sulaimani, Sulaymaniyah, Iraq:119 pp.

[23] Dartash, N.M.O. (2012). Hydrogeology and geoelectrical studies of groundwater in part of Chamchamal area Kurdistan region NE-Iraq, M.Sc. thesis, University of Sulaimani, Sulaymaniyah, Iraq: 144 pp.

[24] Buday, T. (1980). The Regional Geology of Iraq, Vol. I. Stratigraphy and Paleogeography. I.I.M. Kassab and S.Z.Jassim (Eds). SOM, Baghdad, Dar El Kutib Publ. House, Univ. of Mosul: 445pp.

[25] Siether, A. (2012). Isotopic and Geomicrobiological investigation of Darzila Karst Cave, NE Iraq. Diploma project, Technical university of Freiberg, Freiberg, Germany:151 pp.

[26] Stevanovic, Z. and Markovic, M.(2004b). Hydrogeology of Northern Iraq, General Hydrogeology and Aquifer Systems, Vol.2. Food and Agriculture Organization of the United Nations, Rome: 246 pp.

[27] Heiland, K. (2012). Hydrogeochemical investigation of Darzila karst cave, NE Iraq. Diploma thesis. TU Bergakademie Freiberg. Fakultät für

Geowissenschaften, Geotechnik und Bergbau, Germany: 121 pp.
[28] Al-Hafeed. S.B.I. (2016). Reconstructing of paleoclimate through hydrogeological and environmental studies of Shalaii Cave, SE of Sangaw, Iraqi Kurdistan Region, M.Sc. thesis, University of Sulaimani, Sulaymaniyah, Iraq: 154 pp.
[29] Baba Sheikh, S. M. (2000). Hydrochemistry of cave and spring waters in (Sangaw-Chamchamal), Sulaimani Governance. M.Sc. thesis, Baghdad University, Baghdad, Iraq:123 pp.
[30] Dahlin, T., Bernstone, C. and Loke, M.H. (2002). A 3-D resistivity investigation of a contaminated site at Lernacken, Sweden. *Geophysics*, **67(6)**: 1692-1700. DOI:https://doi.org/10.1190/1.1527070.
[31] Xu, Y., Schoonen, M.A.A., Nordstrom, D.K., Cunningham, K.M., Ball, J.W. (1998). Sulfur geochemistry of hydrothermal waters in Yellostone National Park: I. The origin of thiosulfate in hot spring waters. *Geochem. Cosmochim. Acta*, **62 (23/24)** :3729–2743. DOI:https://doi.org/10.1016/S0016-7037(98)00269-5.
[32] Lauerwald, F., (2007). Sulfur geochemistry of hot springs at Yellowstone National Park - Investigating the importance of sulfur oxidation versus microbial sulfate reduction by species selective sampling and isotopic investigations (Diploma thesis). Universität Bayreuth TU BAF, Germany:115 pp.
[33] Maria, C., 1997. Environmental Sampling and Analysis Lab Manual, CRC Press, Taylor & Francis, USA:373 pp.
[34] Al-Manmi, D.A.M.A.(2018). Environmental isotopes and stochastic modeling study to evaluate Tabin and Sarchnar springs, Kurdistan region-Iraq. *Journal of African Earth Sciences*, **147**:312-321. DOI:https://doi.org/10.1016/j.jafrearsci.2018.06.030.
[35] Federation, W.E., American Public Health Association (APHA). (2017). Standard methods for the examination of water and wastewater. 23th ed. American Public Health Association (APHA), Washington, DC, USA:1545 pp.
[36] Adams, S., Titus, R., Pietersen, K., Tredoux, G. and Harris, C.(2001). Hydrochemical characteristics of aquifers near Sutherland in the Western Karoo, South Africa. *Journal of hydrology*, **241(1-2)**:91-103. DOI:https://doi.org/10.1016/S0022-1694(00)00370-X.
[37] Freeze, R.A., J.A. Cherry. (1979). Groundwater. Prentive-hall, Englewood cliffs, NJ: 604 pp.
[38] Palmer, A. N.; Palmer, M. V. (2004). Sulfate-carbonate interactions in the development of karst. *Northeastern geology and environmental science*, **26 (1)**: 93–106.
[39] Worden, R.H; Smalley, P.C. (1996). H_2S-producing reactions in deep carbonate gas reservoirs: Khuff Formation, Abu Dhabi. *Chemical Geology*, **133**: 157–171. DOI: https://doi.org/10.1016/S0009-2541(96)00074-5.
[40] Machel, H.G. (2001). Bacterial and thermochemical sulfate reduction in diagenetic settings - old and new insights. *Sedimentary Geology*, **140 (1-2)**: 143–175. DOI: https://doi.org/10.1016/S0037-0738(00)00176-7.
[41] Drever, J.I., (1997). The Geochemistry of natural water, surface and groundwater environments, 3rd ed., Prentice Hall, USA: 436 pp.
[42] Ball, J.W. and Nordstrom, D.K. (2003). WATEQ4F. A computer program for calculating speciation of major, trace and redox elements in natural water. USGS, Open file Report: 91-189.
[43] Palmer, A. N. (2007). Cave geology. Dayton, Ohio: Cave Books:454 pp.
[44] Matthess, Georg. 1994. Lehrbuch der Hydrogeologie. 3rd edn. Berlin: Borntraeger, Germany: 575 pp.
[45] Giménez-Forcada, E. (2010). Dynamic of sea water interface using hydrochemical facies evolution diagram. *Groundwater*, **48(2)**:212-216. DOI: 10.1111/j.1745-6584.2009.00649.x.
[46] Giménez-Forcada, E. Sánchez San Román, F.J. (2015). An Excel macro to plot the HFE-diagram to identify seawater intrusion phases. *Groundwater*, **53(5)**: 819-824. DOI: 10.1111/gwat.12280.

دراسة المياه المعدنية باستخدام الطرق الجيوفيزيائية والهيدروجيوكيميائية في مملحة خويلن ، سنكاو ، السليمانية ، العراق

دياري علي محمد الممنمي ، بختيار قادر عزيز ، ازاد طاهر كريم ، هه لو عبداله عثمان ، سه رخيل هاوري محمد ، هاوبير عطا كريم ، اسعد ابراهيم مصطفى ، هيمن فريق محمد

قسم علم الأرض ، كلية العلوم ، جامعة السليمانية ، السليمانية ، العراق

الملخص

تعتمد قرية خويلين كلياً على المياه الجوفية للاستخدام المنزلي والزراعي، علاوة على إنتاج الملح منها عن طريق مجموعة من برك التبخر. تم استخدام التصوير المقطعي للمقاومة الكهربائية (ERT) والهيدروجيوكيمياء لدراسة نظام وتوزيع الأنواع المختلفة من المياه المعدنية التي تتدفق عبر عدة ينابيع والآبار الموجودة في منطقة محددة لا تتجاوز مساحتها 0.14 كيلومتر مربع. تستخدم المياه ذات الملوحة العالية لإنتاج الملح قبل أكثر من مئات السنين ولحد الان، اما المياه الكبريتية فتتميز برائحتها الكريهة. ان المنطقة مغطاة بتكوين الفتحة الذي يتكون من أربعة أنواع دورات ترسيبية، وهي طبقتين غير نفاذيتين من الحجر الطموي والحجر المارلي، وطبقتان ترسيبتان من الحجر الجيري والجبس والتي تتميز بوجود كسور وتكهفات كثيرة. توضح التصوير المقاومي الحقيقي وجود22 كهف بأحجام مختلفة وفي أعماق مختلفة. تم تصنيفها إلى مجموعتين، عشرة تجاويف تم اكتشافها في طبقات الجبس تظهر مقاومة عالية تتراوح من 350 أوم 0 م إلى 1200 أوم.م، وهي على الأرجح تصنع المسار تحت الأرض للمياه الجوفية الكبريتية. المجموعة الثانية هي اثنا عشر تجاويف تظهر في طبقات الحجر الجيري لتكوين الفتحة وهي تظهر مقاومة منخفضة للغاية تتراوح من 0.4 أوم0 م إلى 4 أوم.م وتشكل مسارًا ممتازًا للمياه الجوفية العالي الملوحة. تُبين من هذه الدراسة بان ERT لها قابلية جيدة لإيجاد الحد الفاصل بين المياه المالحة والمياه الكبريتية.

تبين بان هناك عدة عوامل مهيمنة تؤثر على كيميائية المياه الجوفية هي التملح، ترسيب المعادن، الذوبان، تبادل الكاتيونات اضافة الى تأثيرات التضاريس الموضعية والخلط والجيولوجيا. وقد ثبتت هذه العمليات من نتائج التراكيز الأيونية، ومعاملات التشبع، ومخطط HFE، والنظائر المستقرة للأكسجين والهيدروجين.